

Published in final edited form as:

*Nat Struct Mol Biol.* 2009 February ; 16(2): 151–158. doi:10.1038/nsmb.1551.

## Nucleosomes can invade DNA territories occupied by their neighbors

Maik Engholm<sup>1</sup>, Martijn de Jager<sup>2</sup>, Andrew Flaus<sup>1,3</sup>, Ruth Brenk<sup>4</sup>, John van Noort<sup>2</sup>, and Tom Owen-Hughes<sup>1</sup>

<sup>1</sup>Wellcome Trust Centre for Gene Regulation and Expression, College of Life Sciences, University of Dundee, Dundee, DD1 5EH, UK. <sup>2</sup>Physics of Life Processes, Leiden Institute of Physics, Leiden University, Niels Bohrweg 2, 2333 CA Leiden, The Netherlands. <sup>4</sup>Division of Biological Chemistry and Drug Discovery, College of Life Sciences, University of Dundee, Dundee, DD1 5EH, UK.

### Abstract

Nucleosomes are the fundamental subunits of eukaryotic chromatin. They are not static entities, but can undergo a number of dynamic transitions including spontaneous repositioning along DNA. Since nucleosomes are spaced close together within genomes it is likely that on occasion they approach each other and or collide. Here we have used a dinucleosomal model system to show that the 147bp DNA territories of two nucleosomes can overlap extensively. In the situation of an overlap by 44 bp or 54 bp one histone dimer is lost and the resulting complex can condense to form a compact single particle. We propose a pathway in which adjacent nucleosomes promote DNA unraveling as they approach each other and that this permits their 147bp territories to overlap. These may represent early steps in a pathway for nucleosome removal via collision.

---

In eukaryotic cells genomic DNA exists in the form of a nucleo-protein complex called chromatin 1. The packaging of the genomic DNA imposes a hindrance to most DNA-dependent processes including DNA replication, repair and mRNA transcription. This implies an important role for chromatin structure in the control of many nuclear functions 2,3. The first step in the packaging hierarchy of chromatin is the formation of a nucleosome core particle (NCP) 4. The NCP is commonly defined as a complex comprising 147bp of double stranded DNA and an octamer of core histone proteins 5. The core particle as a whole possesses a pseudo-twofold symmetry with the pseudodyad axis passing through the central base pair of the 147bp DNA territory 5,6. It is convenient to refer to this dyad base pair in order to describe the translational position of a nucleosome.

Of great practical and theoretical interest is the question of how the translational positions of nucleosomes on a DNA molecule are specified. Different mechanisms have been proposed. In the case of direct positioning, the position of a nucleosome is solely determined by its interactions with the underlying DNA 7. In a more complex situation indirect positioning involves binding of a non-histone protein such that it directs the positioning of adjacent nucleosomes 8-10. So far relatively little attention has been paid to the question of whether a first nucleosome is capable of indirectly positioning a second one in a similar manner.

---

Correspondence and requests for materials should be addressed to TOH (t.a.owenhughes@dundee.ac.uk)..

<sup>3</sup>Present address: Department of Biochemistry, NUI Galway, Ireland.

**Authors' Contributions** ME carried out most of the experimental work and data analysis. MdJ and JvN carried out AFM and associated data analysis. AF performed the thermal sliding assays in figure 5. RB assisted with the modeling of dinucleosome structure. ME and TOH designed the experiments and wrote the manuscript.

Instead in assigning nucleosome positions genome-wide it has been assumed that overlap between 147bp territories is not possible.

Mononucleosomes can undergo a range of structural transitions including: transient detachment of DNA from the surface of the histone octamer 11,12, destabilization of histone H2A/H2B dimers 13, reconfiguration of histone dimers as part of a packing interaction between nucleosomes 14, a chiral transition of the entire H3/H4 tetramer 15 and repositioning of histone octamers along DNA 16. Given these numerous ways of adapting to their environment it is not clear what actually happens when two nucleosomes approach or collide. None the less this is likely to be of fundamental importance in regulating access to the underlying genetic information.

Here we have studied the behaviour of *Xenopus laevis* nucleosomes as they approach each other using a dinucleosomal system. We find that nucleosome-DNA interactions dominate over the principle of indirect positioning through a second nucleosome: It is possible to assemble template molecules on which the nucleosomes extensively overlap with respect to their 147bp DNA territories. Moreover, we have used this system to analyse the structure of dinucleosomes. We find that nucleosomes promote the unraveling of DNA from their neighbors. In an extreme situation a territorial overlap of 44 bp is observed and in this case one histone dimer dissociates from the complex enabling it to form a condensed particle.

## Results

### Assembly of dinucleosomes with defined separation

We developed a system for assembling dinucleosomes that involves the using the 601 nucleosome positioning sequence to direct sites of nucleosome assembly with high efficiency 17. Two constructs were designed to result in internucleosome spacing of +48 bp or 0 bp, in other words the central dyads of the nucleosomes were separated by 195 and 147 bp respectively (Fig. 1a). A third construct was designed such that the central base pair of each positioning sequence was separated by only 103 bp such that they overlap by 44 bp (Fig. 1a).

Nucleosome assembly reactions were carried out on all three constructs and the extent of assembly first monitored by native gel electrophoresis (Fig. 1b-d). At lower ratios of octamer:DNA, two species were observed consistent with the assembly of just one nucleosome on either of the two positioning elements (Fig. 1 b-d lanes 2-3). In assembly reactions with octamer:DNA ratios of approximately 2:1 a slower migrating species was predominant consistent with the occupancy of both nucleosome positioning sequences on the same DNA fragment (Fig. 1 b-d lanes 4-5).

Site directed nucleosome mapping was used to determine precisely where histone H4 makes contacts with DNA on these fragments. Briefly, this technique involves mapping the locations of cleavage sites caused as a result of the tethering of a DNA cleaving compound to a specific location on the histone octamer. These can be used to assign the nucleosomal dyad 6. In all cases, cleavage sites were observed to occur only at locations consistent with the position nucleosomes have previously been observed to adopt on the 601 sequence (Fig. 1 e-g) 18. On the (-44bp) construct this involves the assembly of nucleosomes at locations in which the 147bp territories overlap by 44bp (i.e. the dyads are separated by 103bp). As nucleosomes assembled onto this construct at an octamer:DNA ratio of 2 have a discrete mobility in native gel electrophoresis (Fig. 1d lane 5) it is likely that a single species is generated in which normal DNA contacts in the region of the dyad are made simultaneously at both of the positioning sequences on the template. While the data in Figure 1 was

obtained using direct repeats of the 601 sequence, very similar results are observed using inverted repeats of the same sequence (Supplementary Fig. 1).

### Histone composition of model dinucleosomes

We first used native gel electrophoresis to monitor intermediates in dinucleosome assembly. Assembly of the (0bp) construct with substoichiometric octamer, tetramer and hexamer resulted in the generation of doublets with distinct electrophoretic mobility's consistent with the generation of single nucleosomes, hexasomes and tetrasomes respectively (Fig. 2a lanes 2-4 bands 1, 2, 3). Assembly reactions performed at higher histone:DNA ratios enabled species corresponding to dinucleosome, ditetrasome and dihexasome to be identified (Fig. 2a lanes 6-8 bands 4, 5, 7). Furthermore, each remaining intermediate during the assembly of two intact adjacent mononucleosomes can also be identified (Supplementary Fig. 2). When the same analysis is applied to the (-44bp) construct a similar pattern is observed, with the exception that one intermediate between a ditetrasome and the fully assembled species is not detected (Fig. 2b; Supplementary Fig. 2). This indicates that the limit species formed upon assembly on the -44bp construct are missing a histone dimer from one nucleosome, but not the other.

In order to substantiate this hypothesis, we purified chromatin assembled on the dinucleosomal constructs from native gels followed by tryptic digestion and nLC/ESI/MS/MS analysis. We next determined the ratio between H2A/H2B dimer peptides and H3/H4 tetramer peptides on the (0bp) and (-44bp) constructs. Peptides derived from H3 and H4 were present at comparable abundances on both the (0bp) and (-44bp) constructs (Fig. 2c). However, peptides derived from H2A and H2B were present on average 0.72-fold less abundant in material derived from the overlapping construct in comparison to the touching nucleosomes (Fig. 2c). This is best explained by the loss of one H2A/H2B dimer on the (-44bp) construct.

### Structural characterization of dinucleosomes by AFM

To gain further insight as to how the dinucleosomes are arranged, they were subject to atomic force microscopy (AFM). Dinucleosomes reconstituted on the three DNA constructs in Figure 1 were isolated by preparative native-gel electrophoresis, fixed in the absence or presence of  $Mg^{2+}$  ions and imaged using tapping mode AFM (Fig. 3a-f). In the absence of divalent cations on all three DNA constructs two separate particles could be resolved on the majority of templates (Fig. 3 a-c). In the presence of 5 mM  $Mg^{2+}$  the (-44bp) construct appears predominantly as single larger particles while template molecules on the (+48bp) and (0bp) constructs can still be resolved as two individual nucleosomes (Fig. 3d-f). Moreover, the particles in Figure 3f are higher than those observed on the other two DNA constructs (Fig. 3g). Under similar ionic conditions an MNase digest of dinucleosomes on the (-44bp) construct gives rise to a protected fragment of approximately 250 bp in length (Fig. 3h). This shows that in the presence of  $Mg^{2+}$  the (-44bp) template molecules condense to form a structure in which the linker DNA between the two particles is not highly accessible.

The particles observed in Figure 3f possess a similar cross-section but increased height compared to a mononucleosome. Such a structure can most easily be obtained if a stacking interaction is formed between the hexasome and the nucleosome. We have built a model of stacked dinucleosome based on two copies of the crystal structure of the NCP (Fig. 4a). The last 44 bp of the DNA double helix in copy 1 were superimposed with the first 44 bp of the DNA in copy 2. The resulting structure resembles an extended nucleosome in which the DNA forms a continuous superhelix of approximately three turns. This arrangement of the DNA is in good agreement with the observed inaccessibility to MNase digest (Fig. 3h).

To test our model we have analyzed the steric interference between the histone proteins in both copies of the NCP. In the presence of both inner dimers massive van der Waals clashes are observed, which are clearly not compatible with the formation of such a structure (Supplementary Fig. 3a). In fact, the two inner dimers cover almost the same volume (Supplementary Fig. 3c). If, however, the inner dimer is absent from copy 2 of the NCP only minimal van der Waals clashes occur (Supplementary Fig. 3b). In addition, these clashes map to regions of the histone proteins which could easily be rearranged in the process of folding.

### Helical phasing contributes to the folded state

We next repeated the modeling described above for overlap lengths ranging from 3 bp to 60 bp and determined the root mean square deviation (RMSD) of the phosphorus atoms in the segment used for superimposition. When plotted as a function of the overlap length a clear 10bp periodicity of the RMSD becomes apparent (Fig. 4b). This reflects the fact that the DNA in superhelix 2 needs to possess the same rotational frame as the DNA in superhelix 1 so they can be superimposed smoothly. In the situation of a dinucleosome this suggests that a folded particle, in which the DNA describes a continuous superhelix, can only be formed if the dyad-to-dyad distance fulfills certain conditions, i.e. is an integer multiple of the helical repeat length of DNA.

To test this hypothesis chromatin was assembled on (-44bp), (-49bp) and (-54bp) constructs corresponding to neighboring local minima or maxima in Figure 4b. On all of these constructs reconstitution gives rise to a limit species which contains only three H2A/H2B dimers (data not shown). Following gel purification and fixation in the presence of  $Mg^{2+}$  the template molecules were imaged by AFM (Fig. 4c-e). The (-44bp) and (-54bp) constructs typically appear as single larger particles (Fig. 4c+e), while in contrast the (-49bp) construct, showed a markedly different behavior. While some of the template molecules still appeared as single larger particles, on the majority of templates two separate small particles could be distinguished (Fig 4d). Thus, on the (-49bp) construct  $Mg^{2+}$ -induced folding indeed occurs much less efficiently than on the other two constructs, for which the dyad-to-dyad distance coincides with local minima in the model for the folded state.

### Generation of overlapping nucleosomes by repositioning

We next sought to investigate whether nucleosomes that are initially intact and separate can rearrange to overlap with each other during the course of spontaneous nucleosome repositioning. To do this dinucleosomes were assembled onto a 396bp DNA fragment derived from the mouse mammary tumor virus (MMTV) long terminal repeat (LTR) 19. Site-directed mapping shows that in the starting material nucleosomes are present at the +70 (nucA) and -127 (nucB) positions (Fig. 5a). During temperature incubation nucleosomes are lost from the +70 location, but remain present at -127 consistent with previous observations indicating that NucA is shifted at lower temperatures than nucB (refs). In addition, new mapping signals are observed at +22 and -25. The simplest explanation for this is that nucleosomes move from +70 to +22 and -25. Movement of a nucleosome to -25 while the second nucleosome remains at -127 would result in the dyads of these two nucleosomes being separated by only 102 bp such that territories overlap by 44bp. Native gel electrophoresis of mono and dinucleosomes assembled onto this DNA fragment shows that mononucleosomes do not contribute to the mapping signal at the -25 location (Supplementary Fig. 4).

Further support for the spontaneous generation of nucleosomes with overlapping territories on the same DNA molecule was obtained by using AFM. Following temperature incubation and fixation in the presence of  $Mg^{2+}$  a considerable proportion of dinucleosomes assembled

on the MMTV fragment appear as single larger particles similar to those formed on the (-44bp) construct (compare Fig. 5b and 3f). In order to assess the occurrence of these particles quantitatively, particle volumes were determined from images obtained before and after mobilization (Fig. 5c+d). The volume distributions observed suggest initially separate nucleosomes form condensed particles similar to those observed on the (-44bp) construct (Fig 5c-g). In concert these observations suggest that spontaneous repositioning can result in collisions between nucleosomes that involve DNA being shared between the two nucleosomal particles

It has been shown previously that SWI/SNF remodeling of nucleosomal arrays gives rise to nucleosomal species that protect 190-250 bp of DNA following digestions with MNase (refs). In combination with our finding in Fig. 3h this raises the possibility that at least some of the products result from the movement of nucleosomes into positions in which the territories overlap. As a first step towards investigating this, dinucleosomes on the MMTV LTR fragment were incubated with increasing amounts of RSC and subjected to site-directed mapping (Fig. 5h). Following remodeling, new mapping signal is observed predominantly at three positions (+18, -62 and -88). If two nucleosomes were present at +18 and at either of the other two positions concomitantly this would result in a territorial overlap of 67 bp or 41 bp. Unfortunately, as the spectrum of products generated following ATP-dependent remodeling are complex involving both nucleosomes moving from their initial locations it is not possible to assign their structure in as much detail as is possible during generation of overlapping nucleosomes by assembly or during spontaneous repositioning.

## Discussion

Nucleosomes are not static entities, but can undergo a number of dynamic transitions including the transient dissociation of the outer turns of DNA and repositioning along DNA 11,16,20. The observations we present here support a simple pathway in which these two properties combine. As a nucleosome moves towards a neighbor the unraveling of DNA at the interface is stabilized such that one nucleosome can invade the DNA territory of another.

Our results demonstrate that both in reconstitution and in repositioning reactions certain DNA sequences induce the formation of overlapping nucleosomes. Consistent with this the DNA sequences upon which we observe dinucleosomes are made up from two separate positioning elements both of which are also functional on their own, i.e. induce a mononucleosome at a defined dyad position. However, we do not believe there is a large penalty or benefit associated with the formation of overlapping nucleosomes for the following reasons. Firstly, if there was a penalty associated with formation of overlapping nucleosomes, we would anticipate that most template molecules would first become occupied by mononucleosomes with overlapping nucleosomes only assembling once each molecule was occupied by one nucleosome. Instead we observe that monomers and overlapping nucleosomes are formed at the same rate regardless of whether the template directs assembly of separate or overlapping nucleosomes (fig 1; data not shown). Secondly, if there was a penalty associated with the formation of overlapping nucleosomes a longer time course or higher temperature would be anticipated when a nucleosome moves to a location coincident with a neighbor in comparison to when it moves to the same location on free DNA. Instead we find that NucA repositions at the same rate in the presence or absence of NucB (not shown).

It has been shown that the positions of nucleosomes in native chromatin at least in part are also selected by the quality of the nucleosome-DNA interactions 21. This raises the possibility that overlapping nucleosomes can also be formed inside a living cell namely in

places where two positioning elements occur at a suitable distance along the genomic DNA. Several recent studies that have assigned nucleosome positions across genome segments have relied on a territorial exclusion principle whereby two neighboring positioning elements cannot be used at the same time if the 147bp territories of the corresponding nucleosomes overlap 21-25. Our results indicate that this restriction is not justified and that instead an overlap of at least 54bp is possible. Other studies focus on the use of nucleosomal DNA of 147bp in length to assign nucleosome positions, when in fact occupancy over a range from 80 – 300bp may be possible 26.

For all DNA constructs characterized by AFM, the measured CM-CM distances indicate that the stretch of DNA physically present between the two nucleosomes is larger than the amount of DNA between their 147bp DNA territories (Supplementary Fig. 5g). It is unlikely that this is simply an artifact occurring during sample preparation as nucleosomes were fixed with glutaraldehyde prior to deposition. Furthermore, the extent of separation was dependent on the ionic conditions in solution at the time of cross-linking and persists at millimolar  $Mg^{2+}$  concentrations (compare Supplementary Fig. 5a+b and d+e). Previous studies have also reported larger than anticipated CM-CM distances at low ionic strength 27-30. The surprisingly large separation between nucleosomes is best explained by the partial unwrapping of nucleosomal DNA. Transient unwrapping of the outer turns of nucleosomal DNA has been observed in mononucleosomes 11,12. The binding of transcription factors to sequences on the edge of nucleosomes acts to promote the unraveling of DNA 20,31 and it is possible that the of neighboring nucleosomes may promote the exposure of DNA in a similar way. This could occur by steric occlusion or electrostatic repulsion. Consistent with the latter, ionic conditions at the time of cross-linking influence CM-CM distances (Compare Supplementary Fig. 5a+b and d+e). The end result is that whereas DNA within a mononucleosome spends approximately 10% of time in the unwrapped state 12, this may be considerably extended in the context of dinucleosomes or longer arrays of uncondensed chromatin.

The dissociation of 3 helical turns of DNA results in the loss of many of the contacts with the histone dimer on that side of the nucleosome. As histone dimers spontaneously dissociate from octamers at physiological salt concentrations, the unraveling of DNA could promote the loss of histone dimers. This will expose an additional proportion of the DNA territory at the interface. If this is subsequently occupied by an adjacent nucleosome reassociation of the dimer would no longer be trivial. This provides a simple pathway by which a nucleosome could invade the DNA territories of its neighbor as a result of spontaneous or ATP-driven repositioning.

On some of the dimeric 601 constructs the two nucleosomes coalesce upon addition of  $Mg^{2+}$  to form particles with a circular cross-section and increased height compared to single nucleosomes. Moreover, overlap lengths, for which  $Mg^{2+}$ -induced folding occurs most readily, recur with a 10bp periodicity and the DNA in the linker region is protected from digestion by MNase. Altogether these observations are indicative of a cylinder-shaped particle with DNA wrapped around its lateral surface in one continuous superhelix. With the aid of the NCP structure we have been able to build a detailed model that fits the experimental observations. The model obtained for a 44bp or 54bp overlap length contains one inner dimer. Although this dimer formally can be assigned to one of the two NCP's it might interact with both tetramers in a structurally equivalent manner (Supplementary Fig. 3c).

For the non-overlapping dinucleosomes on the (0bp) construct it is also possible to obtain a model of a stacked particle, in which only minor steric interference occurs (not shown). Experimentally, however, upon addition of  $Mg^{2+}$  no coalescence of the nucleosomes on

these template molecules can be observed (Fig. 3e) although some compaction has previously been reported by analytical ultracentrifugation 32. This could suggest that two nucleosomal ends, both of which are sealed off by a histone H2A/H2B dimer, generally cannot form the type of stacking interaction required for dinucleosomal folding or association *in trans*. Only when at least one of the two inner dimers is released is a suitable dimerization interface created. This stacking interaction is somewhat reminiscent of previous studies showing that tetramers can stack against each other 6,33,34. Indeed, it is possible that with even greater overlaps than we have studied here adjacent hexasomes might stack in this way.

Chromatin remodeling complexes such as RSC and SWI/SNF use energy derived from ATP hydrolysis to overcome thermodynamic constraints on nucleosome mobility. As a result they have the potential to drive the formation of overlapping nucleosomes even in the absence of suitable positioning elements. Remodeling of mononucleosomes by RSC or SWI/SNF can result in the unraveling of up to 50 bp from the edge of one of these nucleosomes 35-37. The exposed DNA binding surface of these remodeled mononucleosomes provides a means by which they may associate to form dinucleosome-like particles 38,39. Nucleosomes located within arrays do not have the same opportunity to encounter DNA ends. Instead it is far more likely that one nucleosome will collide with a neighbor as a result of sliding. If DNA is unraveled from either nucleosome at the point of collision the result would be that one nucleosome would encroach upon territory occupied by the other in a fashion very similar to that we have reported here.

More recently, generation of an altered dinucleosome like particle, termed the altosome, as a result of SWI/SNF-remodeling of polynucleosomal arrays has been reported 40,41. The altosome differs from the structures we have detected in there is a DNA cross-over between adjacent intact nucleosomes, all histone polypeptides are retained. The hallmark of the altosome is the protection of DNA fragments from 190 to 250 bp in an MNase digest. The latter observation is consistent with the continuous DNA superhelix in our model, but less likely for any arrangement of the DNA that involves a cross-over. While evidence is presented that no histone dimers are lost from altosomes 41 other studies have found that SWI/SNF related complexes reduce the stability with which histone dimers are retained in nucleosomes 42,43, and in this study we found detection of a 25% reduction in histone dimer content to be technically challenging.

Finally, we observed the redistribution of dinucleosomes to positions in which they appear to overlap following remodeling with RSC (Fig. 5h). Therefore, overlapping dinucleosomes may contribute to the spectrum of products generated during the course of ATP-dependent chromatin remodeling reactions. As we also observed that the formation of overlapping nucleosomes can result in the dissociation of histone subunits, it is tempting to speculate that similar species generated during remodeling by SWI/SNF complexes could represent intermediates in the complete removal of histone octamers. In such a reaction an adjacent nucleosome would be required for octamer removal, a concept that is gaining support 44-46 and that is consistent with the observed kinetics of nucleosome removal at the PHO5 promoter 47. It is now important to establish whether they are indeed formed *in vivo*. Our preliminary efforts with this aim have been unsuccessful and it may not be trivial to detect such species if they exist transiently. It is none the less also possible that other DNA translocating enzymes such as DNA and RNA polymerases may precipitate related collisions between nucleosomes.

As collisions between nucleosomes have the potential to perturb chromatin structure on a genome wide scale, it may be generally advantageous to prevent such collisions occurring. All eukaryotes possess nucleosome spacing enzymes including members of the ISWI and

Chd1 families of Snf2 related proteins that act to position nucleosomes equidistant from their neighbors. Many of these enzymes are abundant and have the potential to hydrolyze large quantities of ATP. That they have proven to be of value throughout the evolution of eukaryotes may reflect the importance of preventing inter nucleosome collisions over the majority of our genomes.

## Methods

**DNA fragments**—All dimeric 601 constructs are based on the 147bp core of the 601 sequence as defined in14. The two halves are joined via an *EcoRI* restriction site. Where additional DNA is present it is derived from the DNA flanking the 147bp core in the original 220bp 601 sequence48. Direct-repeat constructs were cloned in pBluescriptII and then PCR-amplified. Indirect-repeat constructs were synthesised by preparative ligation. The MMTV DNA sequences used were amplified from pAB438 49 by PCR such that 18bp extensions were generated on the ends protruding beyond NucA and NucB.

**Nucleosome Reconstitution, native-gel electrophoresis and site-directed hydroxyl-radical mapping**—Expression of histone proteins, octamer refolding and nucleosome assembly were performed as described in50. For mapping experiments H4S47C and H3C110A mutant histones were used. Native-gel analysis and site-directed mapping were performed as described in36. In the experiments in figure 1, 2, S1 and S2 a Cy5 fluorescent end label was used instead of <sup>32</sup>P. These gels were scanned using an FLA-5100 imager (Fuji). RSC complex was purified as described previously 51.

**Mass spectrometry**—Gel slices containing the dinucleosomal species of interest were excised from a native gel and an in-gel tryptic digest was performed. Peptides were extracted from the gel slices and analysed in triplicate by nLC/ESI/MS/MS on an LTQ Orbitrap XL mass spectrometer. For all peptides identified in a Mascot search the signal intensities were obtained by extracted ion chromatograms using the Quan Browser software (Xcalibur). Peptides with a signal intensity of less than 50,000 counts\*seconds were discarded. The remaining signal intensities were normalised by dividing sample by reference for each individual peptide. Each replicate of the sample was divided by each replicate of the reference and the geometric mean was determined. Peptides with a standard deviation of larger than 0.4 were excluded from further analysis. Averaged normalised signal intensities were plotted against peptide number and the geometric mean was calculated separately for the set of dimer-derived and tetramer-derived peptides. Sequences of the peptides used in figure 2c are available on request.

**Atomic Force Microscopy**—Dinucleosomes were purified by native-gel electrophoresis and electroelution. 2µl of the electroeluted samples were fixed in 10µl 5mM Hepes, and 2µl 1% v/v glutaraldehyde for 15 min. Where indicated MgCl<sub>2</sub> was present at a final concentration of 5mM in the fixation reaction. Directly after fixation, 2µl of the mixture was deposited on freshly cleaved mica, flushed with milli-Q water, dried in a stream of nitrogen gas, and imaged using a Nanoscope IV (Digital Instruments) operated in tapping mode AFM, acquiring 1µm\*1µm images with 512\*512 pixels. Image processing was done with custom built software written in LabVIEW.

**Model construction**—All in silico models of dinucleosomes were created in pymol. The models are based on the high-resolution crystal structure of the NCP 1KX5. For superimposition of DNA helices the phosphorus atoms in both strands were used. Construction of the model of the unfolded state of a dinucleosome in figure 5a is described separately in supplement 5.



## Supplementary Material

Refer to Web version on PubMed Central for supplementary material.

## Acknowledgments

We would like to thank Douglas Lamont and Kenneth Beattie for assistance with mass spectrometry and David Norman for assistance with modeling. We thank members of the TOH lab for valuable suggestions. MdJ and JvN were financially supported by the 'Netherlands Organisation for Scientific Research' (NWO) and the European Science Foundation (ESF). ME (Studentship), AF and TOH were funded by the Wellcome Trust (Senior Fellowship 064414).

## References

1. van Holde, KE. Chromatin. Springer-Verlag; New York: 1988.
2. Groth A, Rocha W, Verreault A, Almouzni G. Chromatin challenges during DNA replication and repair. *Cell*. 2007; 128:721–733. [PubMed: 17320509]
3. Workman JL. Nucleosome displacement in transcription. *Genes and Development*. 2006; 20:2009–2017. [PubMed: 16882978]
4. Kornberg RD, Lorch Y. Twenty-five years of the nucleosome, fundamental particle of the eukaryote chromosome. *Cell*. 1999; 98:285–94. [PubMed: 10458604]
5. Davey CA, Sargent DF, Luger K, Maeder AW, Richmond TJ. Solvent mediated interactions in the structure of the nucleosome core particle at 1.9 a resolution. *J Mol Biol*. 2002; 319:1097–113. [PubMed: 12079350]
6. Flaus A, Luger K, Tan S, Richmond TJ. Mapping nucleosome position at single base-pair resolution by using site-directed hydroxyl radicals. *Proc Natl Acad Sci U S A*. 1996; 93:1370–5. [PubMed: 8643638]
7. Widlund HR, et al. Identification and characterization of genomic nucleosome-positioning sequences. *Journal of Molecular Biology*. 1997; 267:807–817. [PubMed: 9135113]
8. Roth SY, Dean A, Simpson RT. Yeast  $\alpha 2$  Repressor Positions Nucleosomes in TRP1/ARS1 Chromatin. *Mol. Cell. Biol*. 1990; 10:2247–2260. [PubMed: 2183026]
9. Strauss F, Varshavsky A. A protein binds to a satellite DNA repeat at three specific sites that would be brought into mutual proximity by DNA folding in the nucleosome. *Cell*. 1984; 37:889–901. [PubMed: 6540146]
10. Pazin MJ, Bhargava P, Geiduschek EP, Kadonaga JT. Nucleosome mobility and the maintenance of nucleosome positioning. *Science*. 1997; 276:809–12. [PubMed: 9115208]
11. Polach KJ, Widom J. Mechanism of protein access to specific DNA sequences in chromatin: a dynamic equilibrium model for gene regulation. *J Mol Biol*. 1995; 254:130–49. [PubMed: 7490738]
12. Li G, Levitus M, Bustamante C, Widom J. Rapid spontaneous accessibility of nucleosomal DNA. *Nat Struct Mol Biol*. 2005; 12:46–53. [PubMed: 15580276]
13. Ferreira H, Somers J, Webster R, Flaus A, Owen-Hughes T. Histone tails and the H3 alphaN helix regulate nucleosome mobility and stability. *Molecular & Cellular Biology*. 2007; 27:4037–48. [PubMed: 17387148]
14. Schalch T, Duda S, Sargent DF, Richmond TJ. X-ray structure of a tetranucleosome and its implications for the chromatin fibre. *Nature*. 2005; 436:138–141. [PubMed: 16001076]
15. Bancaud A, et al. Nucleosome chiral transition under positive torsional stress in single chromatin fibers. *Mol Cell*. 2007; 27:135–47. [PubMed: 17612496]
16. Meersseman G, Pennings S, Bradbury EM. Mobile nucleosomes--a general behavior. *Embo J*. 1992; 11:2951–9. [PubMed: 1639066]
17. Thastrom A, et al. Sequence motifs and free energies of selected natural and non-natural nucleosome positioning DNA sequences. *J Mol Biol*. 1999; 288:213–29. [PubMed: 10329138]
18. Dorigo B, Schalch T, Bystricky K, Richmond TJ. Chromatin fiber folding: requirement for the histone H4 N-terminal tail. *J Mol Biol*. 2003; 327:85–96. [PubMed: 12614610]

19. Richard-Foy H, Hager GL. Sequence-specific positioning of nucleosomes over the steroid-inducible MMTV promoter. *EMBO Journal*. 1987; 6:2321–8. [PubMed: 2822386]
20. Li G, Widom J. Nucleosomes facilitate their own invasion. *Nat Struct Mol Biol*. 2004; 11:763–9. [PubMed: 15258568]
21. Segal E, et al. A genomic code for nucleosome positioning. *Nature*. 2006; 442:772–8. [PubMed: 16862119]
22. Yuan GC, et al. Genome-scale identification of nucleosome positions in *S. cerevisiae*. *Science*. 2005; 309:626–30. [PubMed: 15961632]
23. Johnson SM, Tan FJ, McCullough HL, Riordan DP, Fire AZ. Flexibility and constraint in the nucleosome core landscape of *Caenorhabditis elegans* chromatin. *Genome Research*. 2006; 16:1505–1516. [PubMed: 17038564]
24. Albert I, et al. Translational and rotational settings of H2A.Z nucleosomes across the *Saccharomyces cerevisiae* genome. *Nature*. 2007; 446:572–6. [PubMed: 17392789]
25. Lee W, et al. A high-resolution atlas of nucleosome occupancy in yeast. *Nat Genetics*. 2007; 39:1235–44. [PubMed: 17873876]
26. Fatemi M, et al. Footprinting of mammalian promoters: use of a CpG DNA methyltransferase revealing nucleosome positions at a single molecule level. *Nucleic Acids Research*. 2005; 33:e176. [PubMed: 16314307]
27. Allen MJ, et al. Atomic force microscope measurements of nucleosome cores assembled along defined DNA sequences. *Biochemistry*. 1993; 32:8390–6. [PubMed: 8357790]
28. Pisano S, Pascucci E, Cacchione S, De Santis P, Savino M. AFM imaging and theoretical modeling studies of sequence-dependent nucleosome positioning. *Biophysical Chemistry*. 2006; 124:81–9. [PubMed: 16824667]
29. van Holde K, Zlatanova J. The nucleosome core particle: does it have structural and physiologic relevance? *Bioessays*. 1999; 21:776–780. [PubMed: 10462418]
30. Thoma F, Koller T, Klug A. Involvement of histone H1 in the organization of the nucleosome and of the salt-dependent superstructure of chromatin. *J. Cell Biol*. 1979; 83:403–427. [PubMed: 387806]
31. Polach KJ, Widom J. A model for the cooperative binding of eukaryotic regulatory proteins to nucleosomal target sites. *J Mol Biol*. 1996; 258:800–12. [PubMed: 8637011]
32. Butler PJG, Thomas JO. Dinucleosomes show compaction by ionic strength, consistent with bending of linker DNA. *Journal of Molecular Biology*. 1998; 281:401–407. [PubMed: 9698556]
33. Alilat M, Sivolob A, Revet B, Prunell A. Nucleosome dynamics IV. Protein and DNA contributions in the chiral transition of the tetrasome, the histone (H3-H4)(2) tetramer-DNA particle. *Journal of Molecular Biology*. 1999; 291:815–841. [PubMed: 10452891]
34. Tomschik M, Karymov MA, Zlatanova J, Leuba SH. The archaeal histone-fold protein Hmf organizes DNA into bona fide chromatin fibers. *Structure*. 2001; 9:1201–11. [PubMed: 11738046]
35. Fan HY, He X, Kingston RE, Narlikar GJ. Distinct strategies to make nucleosomal DNA accessible. *Mol Cell*. 2003; 11:1311–22. [PubMed: 12769854]
36. Flaus A, Owen-Hughes T. Dynamic properties of nucleosomes during thermal and ATP-driven mobilization. *Mol Cell Biol*. 2003; 23:7767–79. [PubMed: 14560021]
37. Kassabov SR, Zhang B, Persinger J, Bartholomew B. SWI/SNF unwraps, slides and rewraps the nucleosome. *Molecular Cell*. 2003; 11:391–403. [PubMed: 12620227]
38. Lorch Y, Zhang M, Kornberg RD. RSC unravels the nucleosome. *Mol Cell*. 2001; 7:89–95. [PubMed: 11172714]
39. Ulyanova NP, Schnitzler GR. Inverted factor access and slow reversion characterize SWI/SNF-altered nucleosome dimers. *Journal of Biological Chemistry*. 2007; 282:1018–1028. [PubMed: 17121825]
40. Schnitzler GR, et al. Direct imaging of human SWI/SNF-remodeled mono- and polynucleosomes by atomic force microscopy employing carbon nanotube tips. *Mol Cell Biol*. 2001; 21:8504–11. [PubMed: 11713285]

41. Ulyanova NP, Schnitzler GR. Human SWI/SNF generates abundant, structurally altered dinucleosomes on polynucleosomal templates. *Mol Cell Biol.* 2005; 25:11156–70. [PubMed: 16314535]
42. Bruno M, et al. Histone H2A/H2B dimer exchange by ATP-dependent chromatin remodeling activities. *Mol Cell.* 2003; 12:1599–606. [PubMed: 14690611]
43. Vicent GP, et al. DNA instructed displacement of histones H2A and H2B at an inducible promoter. *Mol Cell.* 2004; 16:439–52. [PubMed: 15525516]
44. Cairns BR. Chromatin remodeling: insights and intrigue from single-molecule studies. *Nature Structural & Molecular Biology.* 2007; 14:989–996.
45. Dechassa ML, et al. Architecture of the SWI/SNF-nucleosome complex. *Molecular and Cellular Biology.* 2008; 28:6010–6021. [PubMed: 18644858]
46. Chaban Y, et al. Structure of a RSC-nucleosome complex and insights into chromatin remodeling. *Nat Struct Mol Biol.* 2008; 15:1272–1277. [PubMed: 19029894]
47. Boeger H, Griesenbeck J, Kornberg RD. Nucleosome retention and the stochastic nature of promoter chromatin remodeling for transcription. *Cell.* 2008; 133:716–726. [PubMed: 18485878]
48. Lowary PT, Widom J. New DNA sequence rules for high affinity binding to histone octamer and sequence-directed nucleosome positioning. *J Mol Biol.* 1998; 276:19–42. [PubMed: 9514715]
49. Flaus A, Richmond TJ. Positioning and stability of nucleosomes on MMTV 3' LTR sequences. *Journal of Molecular Biology.* 1998; 275:427–441. [PubMed: 9466921]
50. Luger K, Rechsteiner TJ, Richmond TJ. Expression and purification of recombinant histones and nucleosome reconstitution. *Methods Mol Biol.* 1999; 119:1–16. [PubMed: 10804500]
51. Ferreira H, Flaus A, Owen-Hughes T. Histone modifications influence the action of Snf2 family remodelling enzymes by different mechanisms. *Journal of Molecular Biology.* 2007; 374:563–579. [PubMed: 17949749]

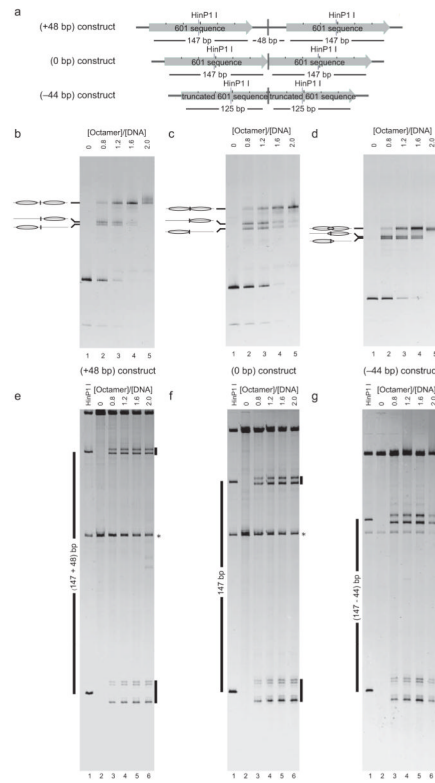


**Figure 1. Chromatin assembly on defined dinucleosomal templates**

**a**, Schematic representation of three dimeric 601 constructs based on direct repeats of the positioning sequence. The 147bp positioning sequence is indicated by the shadowed arrows. On the (-44bp) construct 22 bp have been removed from the inward-looking end of each of the two copies. **b-d**, Native-gel analysis of reconstitutions on the above DNA constructs. Reconstitutions were performed at increasing [octamer]:[DNA] ratios. Bands corresponding to the two types of mononucleosomes and one type of dinucleosome are indicated. **e-g**, Site-directed-mapping analysis of the reconstitutions in (b-d). Mapping signals are indicated by the vertical bars on the right. The marker lanes on the left contain DNA partially digested at the *HinPI* 1 restriction sites 2 bp upstream of the 601 dyad position. The DNA fragments used in the reconstitution reactions were prepared by PCR which also gives rise to some DNA fragments comprising a single repeat of the 601 sequence only (\*).

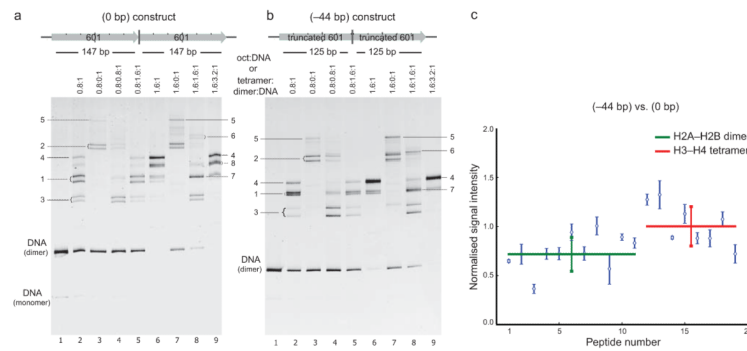


**Figure 2. Measuring the histone content of dimeric chromatin particles**  
**a+b**, Reconstitution and native-gel analysis. Reconstitutions were performed at the indicated [octamer]:[DNA] and [tetramer]:[dimer]:[DNA] ratios and analyzed by means of native-gel electrophoresis. Assembly was performed on **a** the (0bp) and **b** the(-44bp) construct. Each intermediate in assembly is labeled for a full description see text and Supplementary Figure 2. 1, mononucleosomes; 2, monotetrasomes; 3, monohexasomes; 4, fully assembled species; 5, ditetrasome; 6, tetrasome-hexasome; 7 dihexasome; 8 hexasome-nucleosome. **c**, The major fully assembled species (i.e. bands 4 in **a+b**) were purified by native-gel electrophoresis, digested with trypsin and analysed in triplicate by LC/ESI/MS/MS. Signal intensities of peptides in the (-44bp) samples were divided by the corresponding signal intensities in the (0bp) samples and the average over all replicates was calculated for each individual peptide (blue diamonds). Then these averaged normalized signal intensities were averaged separately for dimer-derived (green) and tetramer-derived (red) peptides yielding a [dimer]:[tetramer] ratio of 0.72. Standard deviations are shown as error bars.

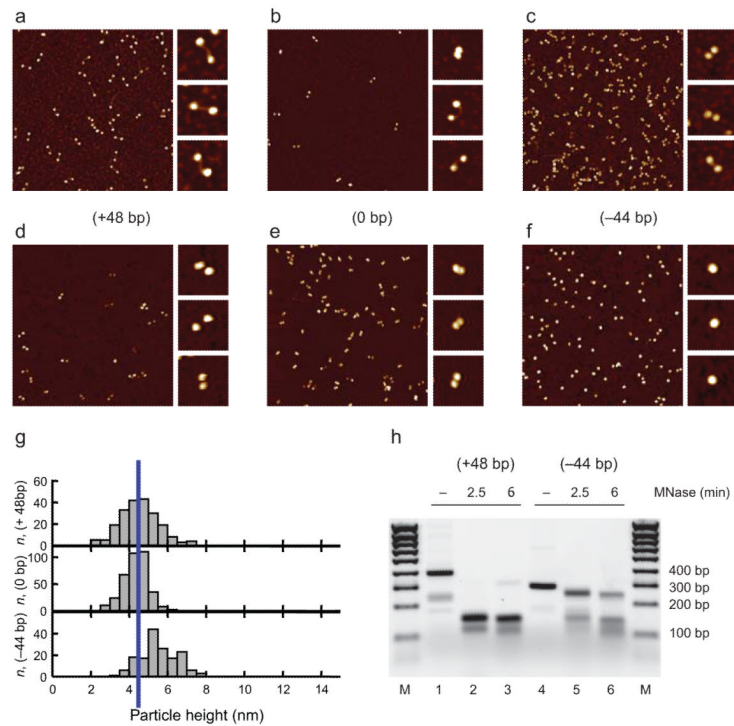


**Figure 3. AFM imaging of dinucleosomes**

**a-f**, Dinucleosomes on the respective constructs were gel-purified, fixed in the absence (**a-c**) or presence (**d-f**) of 5 mM Mg<sup>2+</sup> and imaged. In the presence of divalent cations the overlapping dinucleosomes on the (-44bp) construct appear as single particles of increased height. **g**, Maximal heights of the particles in the experiments in d-f. The average height of the nucleosomes on the (+48bp) and (0bp) constructs is indicated by the blue vertical line. **h**, Dinucleosomes on the (+48bp) (lanes 1-3) and (-44bp) (lanes 4-6) constructs were treated with MNase for the indicated amounts of time. An MNase resistant fragment of around 250 bp is observed for the dinucleosomes on the (-44bp) construct.

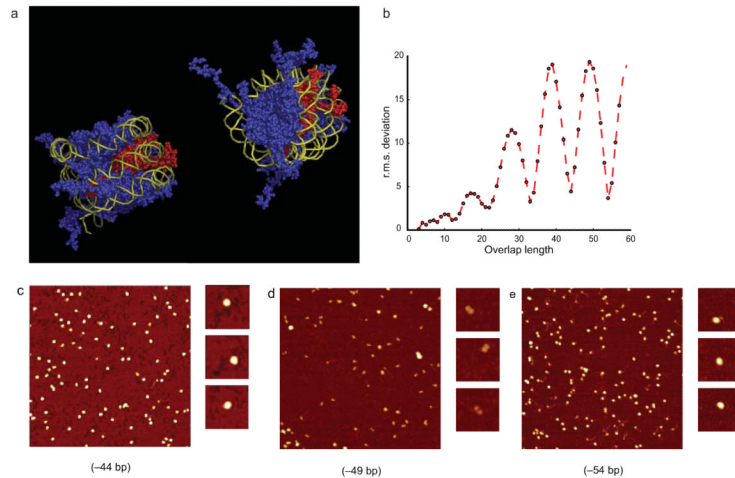


**Figure 4. Helical phasing is required for the condensation of overlapping dinucleosomes**  
 Structural models of dinucleosomes on the (-44bp) construct in the unfolded (left) and folded (right) states (a). The exposed inner dimer on the complete nucleosome is highlighted red. Other histone proteins are shown in blue and DNA in yellow. **b**, A plot of the root mean square deviation (RMSD) of phosphorus atoms as a function of the overlap length for partial superimposition of two copies of the DNA superhelix in 1KX5. For a chosen overlap length  $n$  the last  $n$  base pairs in the first copy were superimposed with the first  $n$  base pairs in the second copy. The helical periodicity suggests that formation of compact structures is likely to require helical phasing. **c-e**, AFM imaging of dinucleosomes with overlaps lengths of -44, -49 and -54 bp following fixation in 5 mM  $Mg^{2+}$ . Formation of compact particles is observed for the (-44bp) and (-54bp) constructs that coincide with minima in **a**, unfolded particles predominate for the -49bp construct.

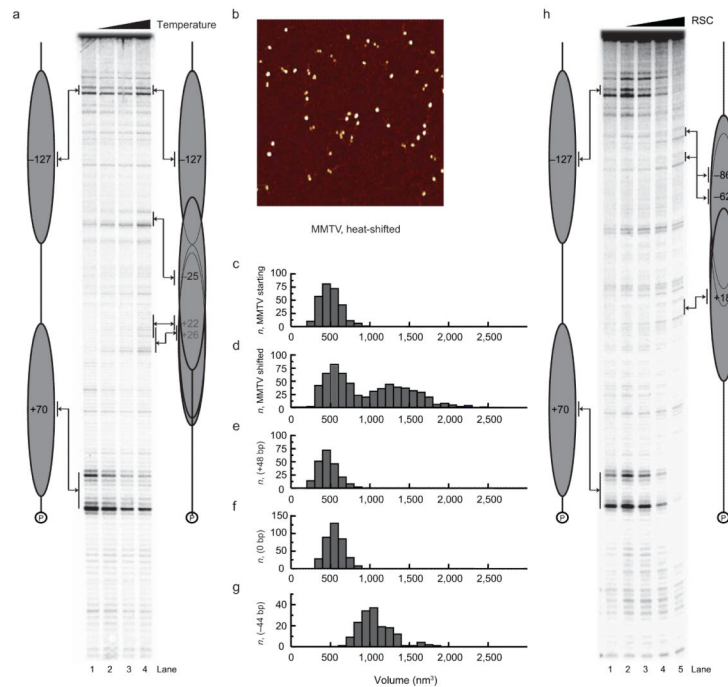


**Figure 5. Formation of overlapping nucleosomes as a result of repositioning**

**a.** Samples of a dinucleosomal reconstitution on the MMTV were incubated at 0, 42, 47 or 52 °C for 60 min and analyzed by site-directed mapping. Mapping signals are labeled with the respective dyad positions. **b.** Dinucleosomes were gel-purified, temperature-treated and fixed in the presence of 5 mM Mg<sup>2+</sup> followed by AFM imaging at room temperature. **c-g.** Volumetric analysis of particles on the MMTV fragment before (**c**) and following (**d**) temperature incubation and on the three 601 constructs in the presence of Mg<sup>2+</sup>. Where two particles could be resolved on a template molecule their volumes were determined and scored separately. Where only one large particle was present the total volume of the composite particle was used. **h** 2 pMoles of Dinucleosomes assembled on MMTV DNA were subject to remodeling with 0, .015, .03, 0.6, .012 fmoles RSC in the presence of 1mM ATP from 30 min at 30°C. Following remodeling the major new locations detected are consistent with nucleosomes moving into locations in which their DNA territories overlap. The loss of mapping signal in lanes 4 and 5 may be due to the increased heterogeneity in the remodeled chromatin and or additional alterations to chromatin structure.